

Received June 20, 2020; reviewed; accepted July 25, 2020

## Effect of particle shape properties on selective separation of chromite from serpentine by flotation

Onur Guven <sup>1</sup>, M. Tayhan Serdengecti <sup>2</sup>, Berivan Tunc <sup>2</sup>, Orhan Ozdemir <sup>3</sup>, Ibrahim E. Karaagaclioglu <sup>4</sup>, Mehmet S. Çelik <sup>2,4</sup>

<sup>1</sup> Adana Alparslan Türkeş Science and Technology University, Faculty of Engineering, Department of Mining Engineering, Adana, Turkey

<sup>2</sup> Istanbul Technical University, Department of Mineral Processing Engineering Department, Istanbul-Turkey

<sup>3</sup> Istanbul University-Cerrahpaşa, Department of Mining Engineering, Buyukcekmece, Istanbul-Turkey

<sup>4</sup> Harran University, Şanlıurfa Technical Sciences, Vocational School, Şanlıurfa-Turkey

Corresponding author: [oguvan@atu.edu.tr](mailto:oguvan@atu.edu.tr) (Onur Guven)

**Abstract:** Although many studies have been conducted on the morphological variations and its effects on flotation recoveries of a single mineral system, a systematic study for the flotation behavior of mixtures of minerals has not dwelled much. In this study, the flotation behavior of chromite and serpentine minerals was investigated to distinguish and isolate the contribution of morphology in single and binary systems. For this purpose, the shape analyses for the minerals ground as single and mixture were performed, and their flotation behaviors determined with the micro-flotation experiments. Additionally, the zeta potential measurements were carried out in the presence of sodium oleate as a collector. The shape analysis of the ground samples showed that while the roundness values of chromite and serpentine (gangue) minerals as single were quite different, the particle shape of chromite favored serpentine in the mixture system which in turn suggested that the mineral with the high hardness value dominates the shape characteristics in binary grinding conditions. Accordingly, while the flotation characteristics of chromite in the mixture followed the same trend with the flotation of a single chromite system as a function of particle shape, almost a reverse trend was obtained for the shape and flotation of serpentine in the mixture compared to a single serpentine system. Thus, at roundness values of chromite particles from 0.797 to 0.732, the flotation recoveries of chromite in the mixture increased from 51.0% to 75.4%. On the other hand, likewise chromite, the flotation recoveries of serpentine increased from 20.0% to 37.3% proportional to the roundness range of 0.757 and 0.709. These findings in turn showed that the grinding conditions dictate the soft component to be monitored by the harder and denser component which dominates the angularity and floatability of the mixture.

**Keywords:** chromite, serpentine, morphology, flotation, mineral mixtures

### 1. Introduction

In recent years, the outcome of size reduction processes, viz. particle morphology has received enormous interest in mineral processing due to its outstanding role in the liberation and subsequent beneficiation processes (Xia and Li, 2015; Guven et al., 2016; Xia et al., 2017; Chen et al., 2018). In this context the optimization of the crushing and grinding process is strongly required to enhance the efficiency of separation depending on liberation size (Sirkeci et al., 2018). Since the liberation of most minerals occurs in fine and very fine size ranges, methods such as flotation that utilizes the wettability differences between valuable and gangue minerals come into a front for their separation.

Many parameters are affecting the efficiency of the flotation process, like pH, medium viscosity, reagent type, dosage, etc. (Bulut et al., 2011). However, besides the effects of these parameters on flotation, particle morphology become crucial in most industrial and lab-scale applications which

induce a significant impact on bubble-particle and particle-particle interactions (Verelli et al., 2014; Guven et al., 2015; Hassas et al., 2016). Thus, the optimization of grinding is the main variable that changes the physical characteristics of minerals such as particle size and morphology (Ulusoy et al., 2003; Yekeler et al., 2004; Rezai et al., 2010). In this manner, control of shape characteristics plays an important role on increasing the flotation recoveries of several types of industrial minerals as quartz (Ulusoy et al., 2003), barite (Ulusoy et al., 2004), chromite (Little et al., 2015), calcite (Ulusoy et al., 2004), talc (Yekeler et al., 2004), wollastonite (Wiese and O'Connor, 2016), chalcopyrite (Vizcarra et al., 2016, Zhang et al., 2020) and malachite (Li et al., 2019). However, to our knowledge, only a few studies have considered the effect of grinding time on both particle shape and flotation recovery values (Guyen et al., 2016; Turk et al., 2018). In particular, the effect of grinding time on shapes of binary mixtures consisting of chromite and serpentine has never been studied.

Many papers can be found on fundamentals of chromite and serpentine flotation including the effects of different reagents (Palmer et al., 1975; Sysila et al., 1996; Guney et al., 1999), modifiers and other relevant conditions (Gallios et al., 2007). However, there is no study directed towards the contribution of particle shape on the flotation separation of these minerals. Considering the lack of knowledge in literature, the aim of this study was to understand the effect of controlled grinding conditions on the morphology of chromite and one of its major gangue mineral "serpentine" on flotation separation of both their individuals and binary mixture under controlled conditions.

## 2. Materials and methods

### 2.1. Materials

Chromite and serpentine samples used in this study were obtained from ETI Krom Inc, Elazig and KUMAS Magnesite Inc., Kutahya, respectively. The crystallinity of the samples was determined by X-Ray Diffractometer Analysis (XRD) using the Bruker D8 Advance XRD unit. The radiation applied was  $\text{CuK}\alpha$  from a long fine focus Cu tube, operating at 40 kV and 40 Ma. The XRD results of the samples revealed that the samples were mainly composed of chromite and serpentine minerals with impurities in trace quantities (Fig. 1).

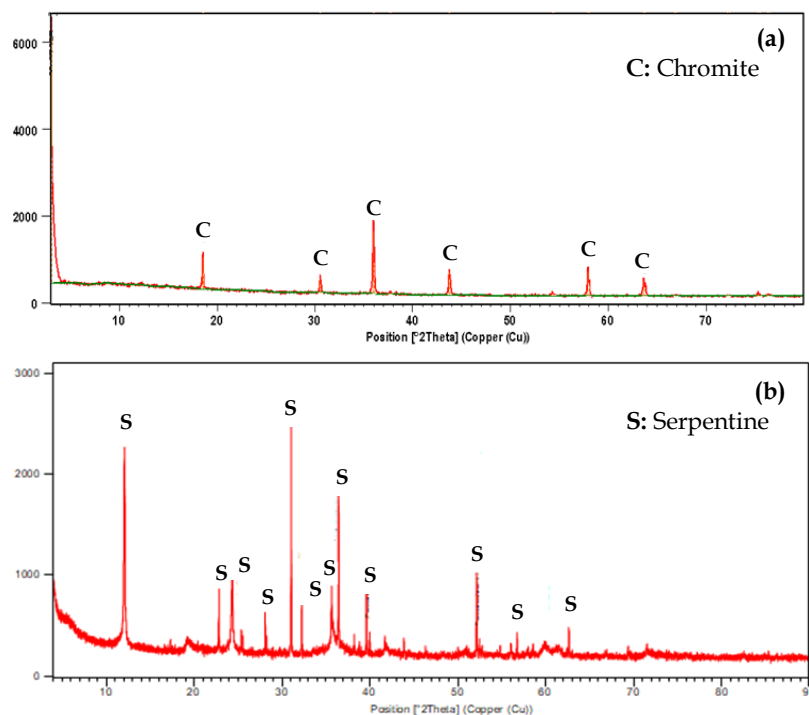


Fig. 1. XRD results of chromite (a) and serpentine (b) samples

For producing suitable feed material for the flotation experiments, the samples over 10 cm were crushed to -1 mm by adopting a series of jaw, cone, and roll crushers. The crushed material was dry

screened with 1, 0.841, 0.710, 0.595, and 0.500 mm sieves to determine the particle size distribution of feed to grinding mill. The size distributions of feed for chromite and serpentine are shown in Fig. 2a. As shown in Fig. 2a, the  $d_{80}$  of crushed samples was very close to 900  $\mu\text{m}$  for chromite and 841  $\mu\text{m}$  for serpentine, respectively. The PSD (Particle Size Distribution) of crushed material indicated that the presence of fines ( $<106 \mu\text{m}$ ) in the feed material was negligible.

Based on the weight of fractions in the crushed sample, the feed size for the grinding was selected - 841+710  $\mu\text{m}$ . The grinding tests were conducted in dry conditions as a function of grinding time (15, 30, 60, 120, 240, 480, and 960 s). In the grinding tests, a mixture of steel balls (which were 30, 25, and 20 mm in diameter and weighed 816 g) were used in a cylindrical laboratory type ball mill of 5224  $\text{cm}^3$  in volume ( $D=19.5 \text{ cm}$ ,  $H=17.5 \text{ cm}$ ). The grinding processes were conducted under dry conditions. During these tests, mill-feed subsamples were ground at different times in the range of 15 to 960 s, after which -106+53  $\mu\text{m}$  was screened off from each grinding step material by dry screening (Fig. 2b). It is worth noting that the fraction was wet screened using the same sieves before the flotation and shape characterization of particles to eliminate the remaining fine-sized particles that could not be removed by the dry screening. The size range was selected as -106+53  $\mu\text{m}$  based on; i) for better evaluation of shape characteristics by image analysis ii) prevent the slime formation which could affect the flotation recoveries and accordingly average value of shape parameters.

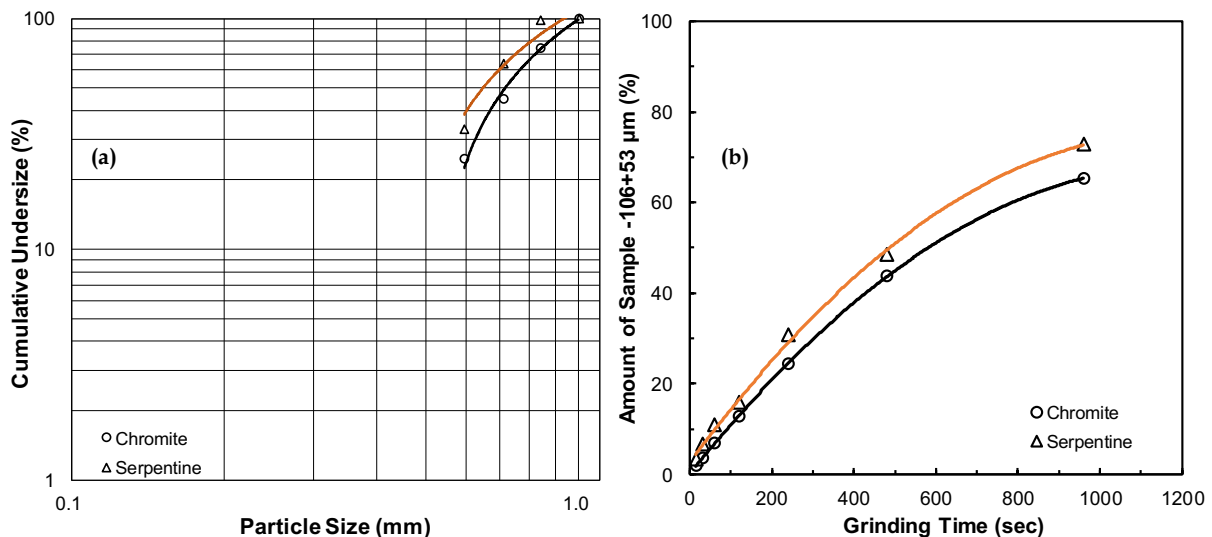


Fig. 2. (a) Particle size distribution of crushed samples (b) amount of particles within -106+53  $\mu\text{m}$  as a function of grinding time

## 2.2. Methods

### 2.2.1. Shape characterization of particles

Due to its ease of application besides other methods such as Fourier analysis (Schwarcz and Shane, 1969; Zhanwei et al., 2014), the shape factors of samples was determined with "Image Analysis" method by using a digital microscope with 50X magnification rate (Güven et al., 2015; 2016). Various shape factors such as relative width, aspect ratio, elongation rate, etc. can be evaluated for particle shape characterization (Ulusoy et al., 2003, 2004; Güven et al. 2015). However, regarding its major role on bubble-particle and particle-particle interactions, only the values of roundness were used for evaluation of particle shape (Güven et al., 2016), the values of roundness parameter were calculated by *Image J* software (Free of License) based on 2-D particle projections obtained from the micrographs of particles (Fig. 3).

The scale of measurement was calibrated before each measurement to obtain accurate and repeatable results for the roundness values calculated by the measured perimeter and the area of particles (Eq. 1). During these measurements, the threshold of each picture was taken by automatic selection based on colors and adjusted settings like the limits of the area, perimeter, etc. Thus, this feature provides an

advantage for giving the ability to work with a number of particles, which is hard to be processed manually. The roundness values were calculated using Eq. 1 (Forsberg and Zhai, 1985):

$$\text{Roundness}(R_o) = \frac{4\pi A}{P^2} \quad (1)$$

where  $P$  is the perimeter, and  $A$  is the area of particle calculated by the software.

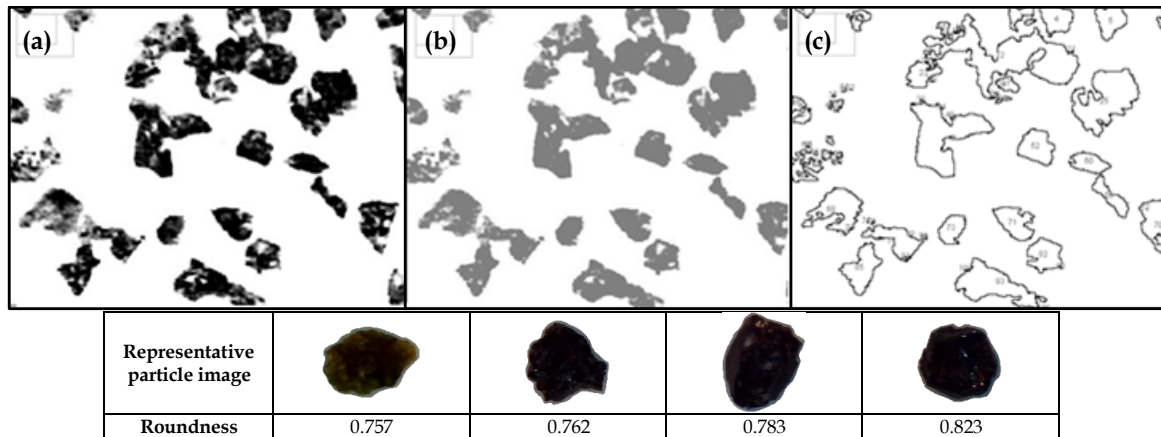


Fig. 3. Image processing steps in *Image J* software, (a) original (b) threshold (c) analyzed

### 2.2.2. Micro-flotation experiments

The micro-flotation experiments were carried out using a 155 cm<sup>3</sup> micro-flotation column cell (30×220 mm) with a ceramic frit (pore size of 15 μm) which was mounted on a magnetic stirrer. High purity nitrogen gas was used for the aeration to maintain the gas flow at a rate of 50 cm<sup>3</sup>/min throughout the flotation experiments. Sodium Oleate (NaOl) (C<sub>18</sub>H<sub>33</sub>NaO<sub>2</sub>,  $M_w$ : 304.44 g) with ≥ 99.0% GC as a collector was supplied from Sigma Aldrich Company.

In the flotation experiments, 1 g of sample was conditioned in the collector solutions at desired concentrations for 3 min. The pH value during these experiments was measured as 8.48±0.03 which was a convenient pH for flotation with NaOl (Gallios et al., 2007). The same procedure was followed during the flotation of mixtures formed by 50% v/v from each mineral. The flotation recovery was calculated based on the weight of floated concentrate (C) to feed (F) (Eq. 2):

$$R = \frac{C}{F} \times 100 \quad (2)$$

### 2.2.3. Zeta potential measurements

Zeta potential measurements were conducted with a microprocessor equipped Zeta-Meter 3.0+ model instrument (Zeta-Meter, USA). The measurements were carried out under 75 V with a cell constant of 0.71 cm<sup>-1</sup>. The procedure for these measurements is as follows: i) the addition of 0.5 g sample (-38 μm) to 50 cm<sup>3</sup> of desired collector concentration (solids ratio 1% w/v) and mixing using a magnetic stirrer at 360 rpm for 5 min, ii) keeping the suspension for 5 min to allow the coarse particles settle down, iii) transfer of the suspension to the measurement cell. Ten measurements at each collector concentration were performed, and the average value of the measurements was obtained for both samples. An average error of measurements was ±2 mV. All measurements were conducted using distilled water, and the pH value of suspensions was measured before and after the measurements, and the natural pH of the suspension was found as 8.48±0.03.

## 3. Results and discussion

### 3.1. Shape characterization of an individual and binary mixture of chromite and serpentine

Many papers are reporting the effect of different parameters on grinding such as grinding media as ball, rod, and autogenous (Ulusoy et al., 2003; Yekeler et al., 2004), ball size (Kim et al., 2019), and dry or wet grinding (Feng and Aldrich, 2000). In these studies, Ulusoy et al. (2003) showed that while rounder quartz particles ( $R_o=0.919$ ) were obtained with ball-milled products it became angular in the case of rod

milled products ( $R_o=0.915$ ). The authors explained this difference by the mechanisms of breakage during the milling process (abrasion, chipping, and impact) for different types of grinding media. In another study of the same group, similar findings were reported for the effects of grinding conditions on talc mineral that while rounder particles were obtained for ball milling ( $R_o=0.922$ ), it became more angular for rod milling process ( $R_o=0.905$ ). In a recent study by Zhang et al. (2020), the effects of grinding media on the morphology of chalcopyrite mineral were investigated by both contact angle measurements and flotation tests. They found that while particles became hydrophobic with contact angle value  $\theta=100.9^\circ$  could be obtained with ceramic balls, they became less hydrophobic with contact angle value of  $\theta=79.8^\circ$  by grinding with cast iron balls. The authors attributed these results to by the variation on roughness values of particles that affect their hydrophobicity. As opposed to chalcopyrite, the results of another recent study indicated that the higher the surface roughness of hydrophilic malachite resulted in higher contact angle values and accordingly higher recoveries in the presence of  $5 \times 10^{-5}$  mol/dm<sup>3</sup> sodium oleate at pH 9 (Li et al., 2019). These results in turn affected their flotation recoveries which will be discussed in further sections.

The various finding was also reported for different minerals grinding systems but to our knowledge, only a few studies have reported the effect of grinding time (Güven et al., 2016; Turk et al., 2018) on morphological variations of particles. For this aim, before the investigation of the effect of grinding of a binary mixture of chromite and serpentine on particle shape, the grinding tests were conducted for each mineral to provide reference points for their grinding characteristics on the shape.

The results shown in Fig. 4 indicated that the range of roundness variation is not wide for chromite and serpentine samples as 0.757-0.828 in comparison to glass beads under the similar grinding conditions (0.980-0.820) or quartz by sand-blasting (0.872-0.672) as reported in the literature (Güven et al., 2015; 2016). However, unlike the decreasing trend in previous studies as a function of grinding time, a sharp drop in the roundness values of chromite (*Zone I*) can be ascribed to the attrition of particles within mill which then abrade rounded corners to sharp ones (0.797-0.762) in the first seconds of grinding (from 15 to 120 s). In foregoing grinding times (120-960 s) removal of sharp corners resulted in rounder ones (0.762-0.823) (*Zones II and III*). In contrary to the chromite sample, while a sharp rise was obtained for serpentine (*Zone I*) in the first seconds of grinding time from 15 to 120 s-(0.792-0.828), it almost remained very close at foregoing grinding times (0.828-0.814) (*Zones II and III*). These variations on shape factors of minerals in turn proved that structural differences showed a significant effect on their grinding patterns.

Following the shape characterization of each mineral, equal volumes of mineral samples were mixed and dry ground under the same conditions (e.g. grinding time, sec) to isolate and distinguish the effect of particle shape on the chromite-serpentine mixture. For analysing the shape variations of each mineral in the mixture, the particles were separated based on their magnetic susceptibility differences with a Frantz Magnetic Separator. The results of these tests are shown in Fig. 5.

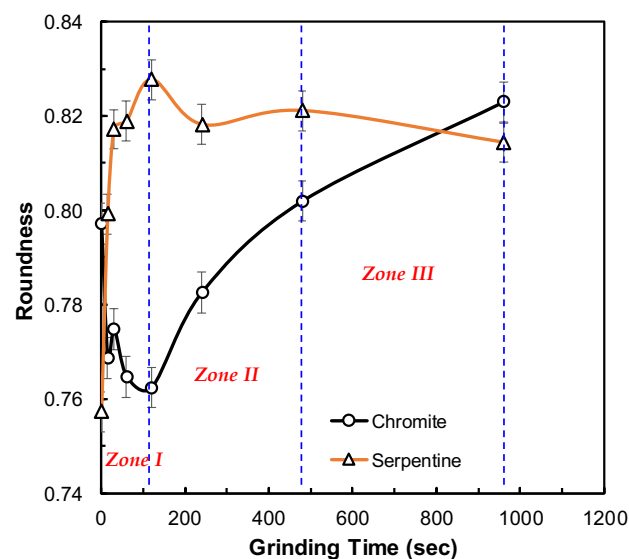


Fig. 4. Effect of grinding on the roundness of chromite and serpentine samples as a function of grinding time

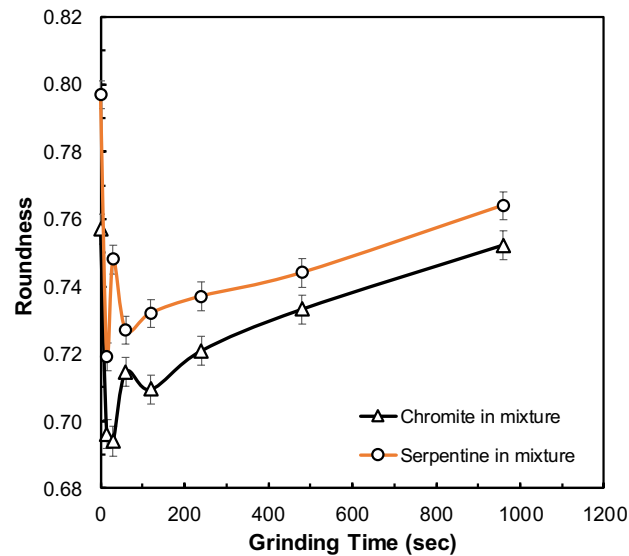


Fig. 5. Effect of grinding on the roundness of chromite and serpentine samples in the binary mixture (50:50 v/v) as a function of grinding time

As shown in Fig. 5 that the roundness values of chromite in the mixture followed the same pattern as observed in previous tests with chromite as a function of grinding time (Fig. 4). Unlike chromite, the roundness values of serpentine in the mixture were found to follow almost the same trend with chromite mineral in the mixture as a function of grinding time. In other words, these findings indicated that while chromite and serpentine (gangue) minerals in their original form behaved quite differently, the particle shape of chromite favoured serpentine in the binary mixture which in turn suggested that the mineral with the high hardness value dominates the shape characteristics in binary grinding conditions. Thus, the above findings made it possible to investigate the effect of roundness on flotation recoveries of individual and mixtures of minerals independently.

### 3.2. Micro-flotation experiments

#### 3.2.1. Effect of Na-Oleate concentration

Prior to the micro-flotation experiments as a function of roundness values, the flotation experiments with single chromite and serpentine minerals were carried out as a function of NaOl concentration at constant roundness values of 0.828 and 0.814 for chromite and serpentine at 960 s grinding time, respectively (Fig. 6). As can be seen in Fig. 6 that while the flotation of chromite was higher at lower concentrations compared to serpentine, the flotation recoveries for both minerals increased with the increase in the collector concentration, and reached the maximum recovery at  $5 \times 10^{-4}$  mol/dm<sup>3</sup>. When the results presented in Fig. 6 are examined carefully, the flotation characteristics of both minerals can be marked by three regions of interest as *Regions I, II, and III*. *Region I* which corresponds to the adsorption of single species on mineral surfaces followed by the breakthrough points which are presumably the onsets of Hemi micellization (*HMC*) occurring around  $5 \times 10^{-5}$  mol/dm<sup>3</sup> for serpentine and  $1 \times 10^{-5}$  mol/dm<sup>3</sup> for chromite.

Above the *HMC*, while a sharp jump-off was obtained for the flotation of serpentine up to  $4 \times 10^{-4}$  mol/dm<sup>3</sup> concentration with 97.9% recovery (*Region II*), the flotation of chromite increased up gradually and ceased at  $5 \times 10^{-4}$  mol/dm<sup>3</sup> concentration with 96.6% recovery in *Region II*. The results for the flotation of both serpentine and chromite with NaOl were found in line with the literature (Palmer et al., 1975; Ucbas et al., 2014). The pH of the medium is another parameter to be considered; while collector uptake appeared to increase at pH values between 2 to 4, it gradually decreased at higher pH values of 4-7 and increased again between pH values 8 and 11 (Palmer et al., 1975). In this context, the adsorption of oleate can be attributed to surface reactions where hydroxyl complexes of Cr<sup>3+</sup> are the controlling mechanisms during flotation. This knowledge of flotation literature guided us to run the flotation experiments at pH  $8.48 \pm 0.03$  to observe and compare the effects of grinding conditions on flotation recoveries of chromite

and serpentine (Gallios et al., 2007). Although the critical micelle concentration (CMC) point of oleate is practically the same for each mineral, the difference in flotation recoveries in *Regions I* and *II* can be explained by the adsorption characteristic of oleate on respective mineral surfaces. Finally, *Region III* exhibits chain-chain interactions which then decreasing the flotation recoveries. Thus, considering their different flotation results, the contribution of shape on the extent of recoveries was investigated by using moderate concentrations as  $8 \times 10^{-5}$  mol/dm<sup>3</sup> and  $1.25 \times 10^{-4}$  mol/dm<sup>3</sup> NaOl (in which 48.06% and 32.36% flotation recoveries obtained for chromite and serpentine, respectively) for chromite and serpentine during subsequent studies.

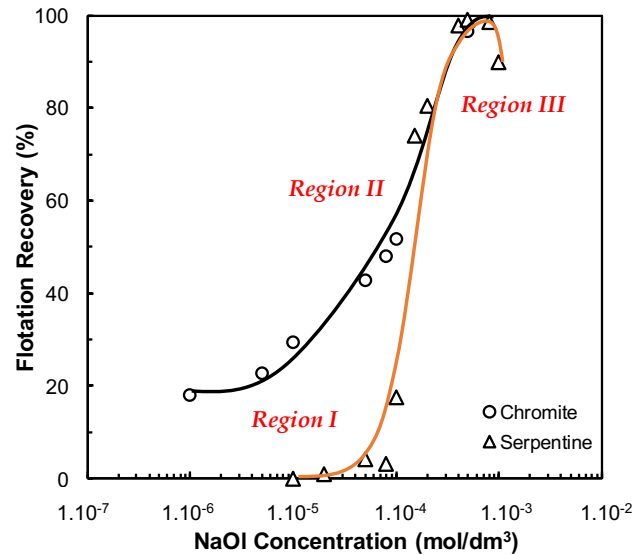


Fig. 6. Effect of collector concentration on the flotation of chromite and serpentine minerals

### 3.2.2. Effect of particle shape

The results of micro-flotation experiments carried out with particles as a function of particle shape which had different roundness values (retrieved from Fig. 2b) are shown in Fig. 7. As can be seen from Fig. 7 that the flotation of each mineral can be divided into two sub-areas based on their roundness values. In the first region, while a gradual increment in flotation recoveries of chromite was obtained up to 60 s of grinding (from 48.06% to 65.79%), a proportional decrement on roundness values was found (0.797-0.7623). Meanwhile, contrary to chromite, while lower flotation recoveries were obtained in the same grinding time range (0-120 sec which corresponded to 32.36-28.09% rec.), a proportional increment on roundness values was found (0.757-0.828). These findings in turn proved the suggestions of many researchers on the effects of angularity on flotation recoveries (Ulusoy et al., 2003; Yekeler et al., 2004; Guven et al., 2015). However, in the following grinding times, although higher roundness values were obtained for both minerals (0.783-0.823 for chromite and 0.818-0.814 for serpentine), significant increases were obtained for the flotation recovery of each mineral. Considering very close PSD values for samples within different grinding times (Fig. 2b), these variations can be ascribed to the possible roughness values of samples which would be extensively explained in future studies. On the other hand, the contribution of roundness and roughness values on flotation recoveries were found in line with the results found for the glass beads (Guyen et al., 2016<sup>a</sup>) and alumina (Guyen et al., 2016<sup>b</sup>) in which similar set up was used.

Considering these results for the flotation of each mineral, the effect of morphology in a binary grinding system of chromite and serpentine was investigated with another series of flotation experiments. In these experiments, in order to maintain a reasonable condition for flotation of each mineral,  $1 \times 10^{-4}$  mol/dm<sup>3</sup> NaOl concentration (in which the flotation recovery was 51% for chromite and 20% for serpentine) was selected, and pH value was adjusted to  $8.48 \pm 0.03$  to mimic the same conditions with the previous experiments. As mentioned in the "Introduction" section, to distinguish the floatability of each type of mineral in a binary mixture, the products of each experiment were analyzed by the Frantz magnetic separator based on their magnetic susceptibilities (Fig. 8).

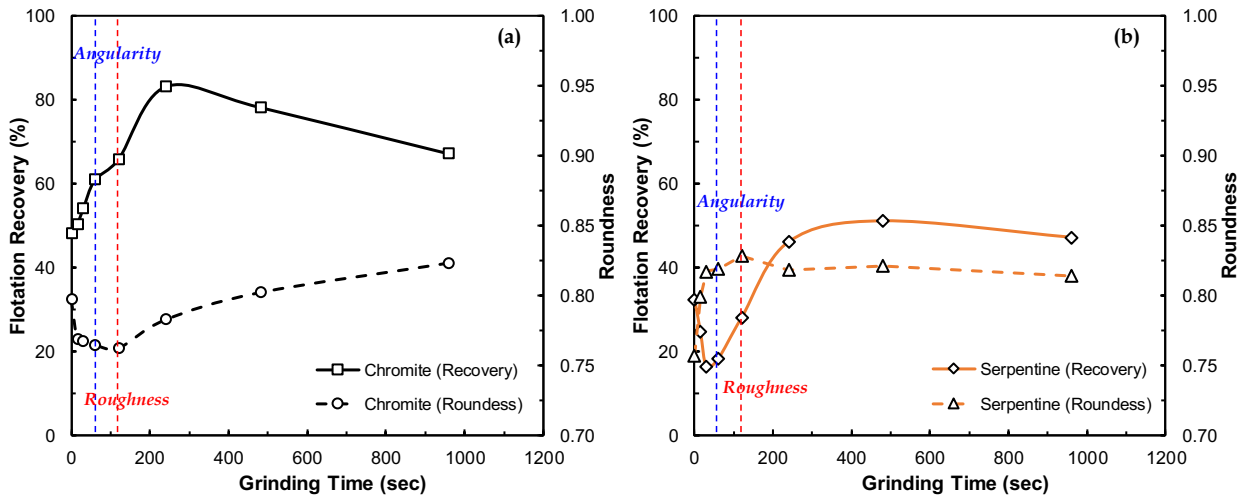


Fig. 7. Effect of grinding time on roundness and flotation recoveries of (a) chromite at  $8 \times 10^{-5} \text{ mol/dm}^3$  (b) serpentine minerals at  $1.25 \times 10^{-4} \text{ mol/dm}^3$  NaOI concentrations

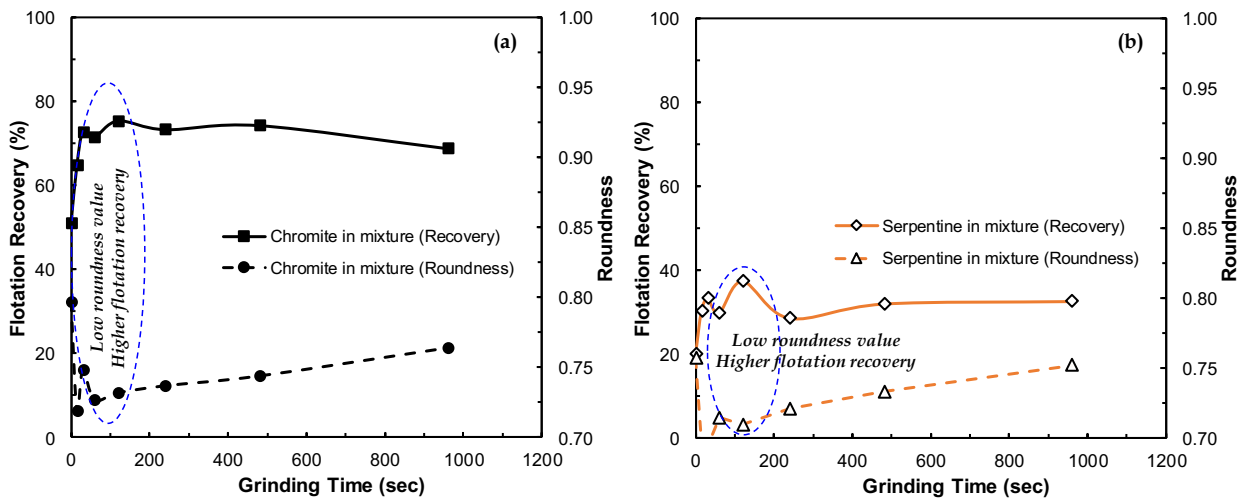


Fig. 8. Flotation recoveries of chromite and serpentine and their mixture at  $1 \times 10^{-4} \text{ mol/dm}^3$  NaOI concentration at  $\text{pH } 8.48 \pm 0.03$

This separation procedure enabled a comparison of the floatability and image analysis of chromite and serpentine individually. The results shown in Fig. 8 revealed that the floatability of both chromite and serpentine followed the same trend with the roundness values of particles in the mixture. On the other hand, these results further indicated for the first time, while chromite in the mixture followed the same path in terms of single flotation results as a function of roundness values, the flotation recovery of serpentine in the mixture varied between 20-38% regardless of its roundness value. These results in turn showed that the particles with high density favour both shape and flotation recoveries in the mixture.

### 3.3. Zeta potential measurements

Figure 9 shows the effect of NaOI concentration on the zeta potential of chromite and serpentine samples at  $\text{pH } 8.48 \pm 0.03$ . As seen in Fig. 9 that up to a certain concentration of NaOI as  $5 \times 10^{-7} \text{ mol/dm}^3$ , while the surface charge of each mineral was positive between +13 and +21 mV, it reversed to negative values which indicates the similar adsorption trend of oleate on their surfaces.

However, if one considers the changes on zeta potential of each mineral, it is clear that while both minerals acquired close values in the concentration range of  $1 \times 10^{-7} \text{ mol/dm}^3$  to  $1 \times 10^{-4} \text{ mol/dm}^3$ , serpentine became more negative at concentrations higher than  $1 \times 10^{-4} \text{ mol/dm}^3$  which can be probably

explained by the chemisorption of oleate on mineral surfaces that may become stronger for serpentine at higher collector concentrations (Sysila et al., 1996; Gallios et al., 2007).

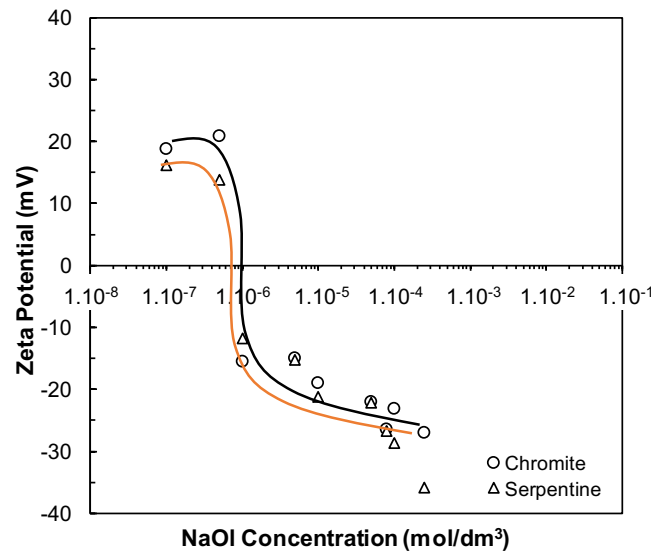


Fig. 9. Effect of collector concentration on zeta potential of chromite and serpentine minerals

#### 4. Conclusions

A systematic grinding procedure was followed for grinding of individual chromite and serpentine minerals and their binary mixture in equal volumes for isolating the effects of grinding conditions in terms of morphological variations. The results of these tests showed that while the morphology of each mineral varied by its inherent physical nature like brittleness or grindability, the particles in the binary mixture were found to follow a trend similar to the one with higher density and hardness, i.e. chromite. In other words, chromite, for the first time, was found to selectively favour the morphological characteristics of particles in a binary mixture with the gangue mineral, serpentine.

Thus, this study provided major information on shape factor-flotation recovery relation in a binary mixture of minerals ground in a ball mill as follows.

While the flotation recovery of individual chromite was measured as 65.8% at 0.762 roundness, it increased to 75% at 0.732 roundness in the binary mixture. Conversely, the roundness of individual serpentine was found to follow an increasing trend up to 120 s of grinding time; this trend was reversed for its flotation recovery. However, in the binary mixture, both the morphological and flotation characteristics of serpentine were found to approach those of chromite. In other words, the roundness of individual serpentine was found as 0.828 but became 0.709 in the case of a mixture, i.e. it became more angular. Consequently, the flotation recovery of individual serpentine was around 28% whereas it increased to 37% in the mixture because of attaining higher angularity. Overall, it appears that the grinding conditions dictate the soft component to be monitored by the harder and denser component which dominates the angularity and floatability of the mixture.

#### Acknowledgement

We are grateful to TUBITAK (Project No.117M659) for supporting this project.

#### References

- BULUT, G., CEYLAN, A., SOYLU, B., GOKTEPE, F., 2011. *Role of starch and metabisulphite on pure pyrite and pyritic copper ore flotation*. Physicochemical Problems of Mineral Processing, 48(1), 39-48.
- CHEN, Y., XIA, W., XIE, G., 2018. *Contact angle and induction time of air bubble on flat coal surface of different roughness*. Fuel, 222, 35-41.
- FENG, D. and ALDRICH, C., 2000. *A comparison of the flotation of ore from the Merensky Reef after wet and dry grinding*. International Journal of Mineral Processing, 60(2), 115-129.

- FORSSBERG, E. and ZHAI, H., 1985. *Shape and surface properties of particles liberated by autogenous grinding*. Scand. J. Metall, 1(14), 25-32.
- GALLIOS, G.P., DELIYANNI, E.A., PELEKA, E.N., MATIS, K.A., 2007. *Flotation of chromite and serpentine*. Separation and Purification Technology, 55, 232-237.
- GUNEY, A, ONAL, G., CELIK, M.S., 1999. *A new flowsheet for processing chromite fines by column flotation and the collector adsorption mechanism*. Minerals Engineering, 12(9), 1041-1049.
- GUVEN, O. and CELIK, M.S., 2016<sup>a</sup>. *Interplay of particle shape and surface roughness to reach maximum flotation efficiencies depending on collector concentration*. Mineral Processing and Extractive Metallurgy, 37(6), 412-417.
- GUVEN, O. KARAKAS, F., KODRAZI, N., CELIK, M.S. 2016<sup>b</sup>. *Dependence of morphology on anionic flotation of alumina*. International Journal of Mineral Processing, 156, 69-74.
- GUVEN, O., CELIK, M.S., and DRELICH, J., 2015. *Flotation of methylated roughened glass particles and analysis of particle-bubble energy barrier*. Minerals Engineering, 79, 125-132.
- GUVEN, O., OZDEMIR, O., KARAAGACLIOGLU, I.E., and CELIK, M.S., 2015. *Surface morphologies and floatability of sand-blasted quartz particles*. Minerals Engineering, 70, 1-7.
- HASSAS, B.V., CALISKAN, H., GUVEN, O., KARAKAS, F., CINAR, M., and CELIK, M.S., 2016. *Effect of roughness and shape factor on flotation characteristics of glass beads*. Colloids and Surfaces A: Physicochemical and Engineering Aspects, 492, 88-99.
- KIM, H.N., KIM, J.W., KIM, M.S., LEE, B.H., KIM, C.J., 2019. *Effects of ball size on the grinding behaviour of talc using a high-energy ball mill*. Minerals, 9, 668, 1-16.
- LI, Z., RAO, F., CORONA-ARROYO, M.A., BEDOLLA-JACUINDE, A., SONG, S., 2019. *Comminution effect on surface roughness and flotation of malachite particles*. Minerals Engineering, 132, 1-17.
- LITTLE, L., BECKER, M., WIESE, J., and MAINZA, A.N., 2015. *Auto-SEM particle shape characterization: Investigating fine grinding of UG2 ore*. Minerals Engineering, 82, 92-100.
- PALMER, B.R., FUERSTENAU, M.C., and APLAN, F.F., 1975. *Mechanisms involved in the flotation of oxides and silicates with anionic collectors*. Part 1. Trans AIME, 258: 261-263.
- REZAI, B., RAHIMI, M., ASLANI, M.R., ESLAMIAN, A., and DEHGHANI, F., 2010. *Relationship between surface roughness of minerals and their flotation kinetics*. In: Proceedings of the XI International Mineral Processing and Technology Congress, 232-238.
- SCHWARCZ, H.P. and SHANE, K.C., 1969. *Measurement of particle shape by Fourier Analysis*. Sedimentology, 13, 213-231.
- SIRKECI, A.A., GUL, A., BULUT, G., OZER, M., GUVEN, O., PEREK, K.T., 2018. *The effect of crushing type on the efficiency of flowing film separation*. Physicochemical Problems of Mineral Processing, 54(2), 601-608.
- SYSILA, S & LAAPAS, H & HEISKANEN, KARI & RUOKONEN, E., 1996. *The effect of surface potential on the flotation of chromite*. Minerals Engineering, 9, 519-525.
- TURK, T., PEREK, K.T., KARAKAS, F., CELIK, M.S., 2018. *Effect of grinding time on particle shape in barite/SDS flotation system*. Proceedings of 16<sup>th</sup> International Mineral Processing Symposium (IMPS 2018), 378-383.
- UCBAS, Y., BOZKURT, V., BILIR, K., IPEK, H., 2014. *Concentration of chromite by means of magnetic carrier using sodium oleate and other reagents*. Physicochemical Problems in Mineral Processing, 50(2), 767-782.
- ULUSOY, U., YEKELER, M., and HICYILMAZ, C., 2003. *Determination of the shape, morphological and their wettability properties of quartz and their correlations*. Minerals Engineering, 16, 951-954.
- ULUSOY, U., HICYILMAZ, C., YEKELER, M., 2003. *Role of shape properties of calcite and barite particles on apparent hydrophobicity*. Chemical Engineering and Processing, 43, 1047-1053.
- VERRELLI, D.I., BRUCKARD, W.J., KOH, P.T.L., SCHWARZ, M.P., and FOLLINK, B., 2014. *Particle shape effects in flotation. Part 1: Microscale experimental observations*. Minerals Engineering, 58, 80-89.
- VIZCARRA, T.G., HARMER, S.L., WIGHTMAN, E. M., JOHNSON, N.W., and MANLAPIG, E.V., 2010. *The effect of breakage mechanism on the mineral liberation properties of sulphide ores*. Minerals Engineering, 23, 374-382.
- WIESE, J., AND O'CONNOR, C., 2016. *An investigation into the relative role of particle size and particle shape and froth behaviour on the entrainment of chromite*. International Journal of Mineral Processing, 156, 127-133.
- XIA, W. and LI, Y., 2015. *Role of roughness on wettability of taixi anthracite coal surface before and after the heating process*. Energy & Fuels, 30, 281-284.
- XIA, W., 2017. *Role of particle shape in the floatability of mineral particle: An overview of recent advances*. Powder Technology, 317, 114-116.

- YEKELER, M., ULUSOY, U., and HIÇYILMAZ, C., 2004. *Effect of particle shape and roughness of talc mineral ground by different mills on the wettability and floatability*. Powder Technology, 140(1-2), 68-78.
- ZHANWEI, Y., FUGUO, L., PENG, Z., BO, C., 2014. *Description of shape characteristics through fourier and wavelet analysis*. Chinese Journal of Aeronautics, 27(1), 160-168.
- ZHANG, X., HAN, Y., GAO, P., LI, Y., 2020. *Effects of grinding media on grinding products and flotation performance of chalcopyrite*. Minerals Engineering, 145, 106070.